SEGMENTATION OF MAGNETIC RESONANCE IMAGES IN PRESENCE OF SEVERE INTENSITY INHOMOGENEITIES

Florian Liebgott[⋆]*, Christian Würslin*[⋆†] *and Bin Yang*[⋆]

[⋆]Institute of Signal Processing and System Theory, University of Stuttgart
[†]Section on Experimental Radiology, University of Tübingen
email: {florian.liebgott, christian.wuerslin, bin.yang}@iss.uni-stuttgart.de

ABSTRACT

In high-field whole body magnetic resonance imaging (MRI), images usually suffer from intensity inhomogeneities. The BC-FAT (bias correction by fitting of adipose tissue intensity) algorithm can compensate for this; however, it is limited to images containing only one object, e.g. the torso. In this paper, we present a method, which extends the BC-FAT algorithm to images containing multiple objects and thus to cross-sectional images of the whole body. This is achieved by an algorithm for the robust and fully automated object detection in MR images using the Hough transform and a modified k-means clustering. We also present a two-scale approach for active contours in order to eliminate the need of object size dependent parametrization for BC-FAT.

Index Terms— whole body MRI, automatic image segmentation, Hough transform, k-means clustering, active contours

1. INTRODUCTION

Computer vision plays an emerging role in medical imaging. Particularly high-resolution morphologic imaging modalities such as computed tomography (CT) and magnetic resonance imaging (MRI) are increasingly combined with automatic or semi-automatic post-processing. Due to the avoidance of ionizing radiation, MRI is widely used in research applications where computer assisted analysis is even more established.

A frequently required task in medical image processing is image segmentation, which can be achieved by finding either homogeneous image areas (e.g. Otsu's method [1], k-means clustering) or boundaries between these areas (e.g. edge detection, active contours [2], level set [3]). The first family of segmentation approaches relies on images in which areas of the same class show constant signal intensity. While this condition is met in CT, MRI may suffer from severe intensity inhomogeneities (IIH).

The reasons for this are twofold: Firstly, the excitation field wavelength of modern high-field MRI systems ($B_0 \geq 3.0\,\mathrm{T}$) is in the range of the measured geometry, causing interference artifacts. Secondly, the frequent use of receive coil arrays to achieve a high spatial resolution results in less homogeneous receive characteristics when compared to large single-channel coils.

These effects contribute to a multiplicative bias field, causing the IIH. It hampers automated image segmentation since different tissue classes heavily overlap in terms of brightness. This renders the application of segmentation methods based on constant threshold impossible. As a possible solution, some methods propose to correct the bias field of the image before segmentation [4], others propose modified clustering schemes accounting for the IIH [5, 6, 7, 8]. However, most of these methods have been developed in the context of neuroscience, where images usually suffer from moderate IIH. They can not cope with severe IIH and are not suited for the whole body.

In [9], an approach called BC-FAT (bias correction by fitting of adipose tissue intensity) for compensating strong bias fields in abdominal image slices has been proposed. The bias field is estimated by fitting areas of adipose tissue (assumed to have constant signal intensity). For the detection of the subcutaneous adipose tissue (SAT), which surrounds the body beneath the skin, active contours (also called snakes) [2] are used. One shortcoming of this method is its restriction to images in which only one single object is present, i.e. to abdominal image slices.

In this paper, we propose the combination of this approach with a newly developed object detection algorithm. This method was tailored to work reliably even in the presence of severe IIH by application of the circular Hough transform. By using the original approach on the determined objects separately, the compensation of inhomogeneities can be applied to cross-sectional MR images of all body parts. In order to fully automate the method, we propose a two-scale approach for the detection of SAT by active contours. With the two-scale approach, the need of object size dependent parametrization for the active contours is eliminated.

2. PROPOSED ALGORITHM

The proposed algorithm, depicted in the flow graph in figure 1, uses circular Hough transform and a modified k-means algorithm to detect objects in MR images. Subsequently, the images are partitioned into subimages containing only one object each.

For the estimation of the inhomogeneities, the BC-FAT algorithm [9] is used. The detection of the SAT ring by snakes and the identification of the sampling points for the estimation of the bias field is performed for each subimage individually. However, the bias field is estimated for the whole image at once using all sampling points of the corresponding subimages.

2.1. Hough transform

Due to the inhomogeneities, the SAT compartments are partially darkened, see figure 2. Hence, it is not always possible to detect the whole SAT ring – and thereby the object contour – with intensity based or edge based segmentation algorithms. Problems arise especially if there are two or more locations on one SAT ring, where the intensity is very low. In this case, intensity or edge based algorithms detect two or more ring segments, which are not connected. Thereby, instead of detecting one object, several objects are detected.

As all transversal cross sections of the human body result in approximately elliptic objects, a Hough transform is used to detect these objects. The Hough transform, originally developed to detect

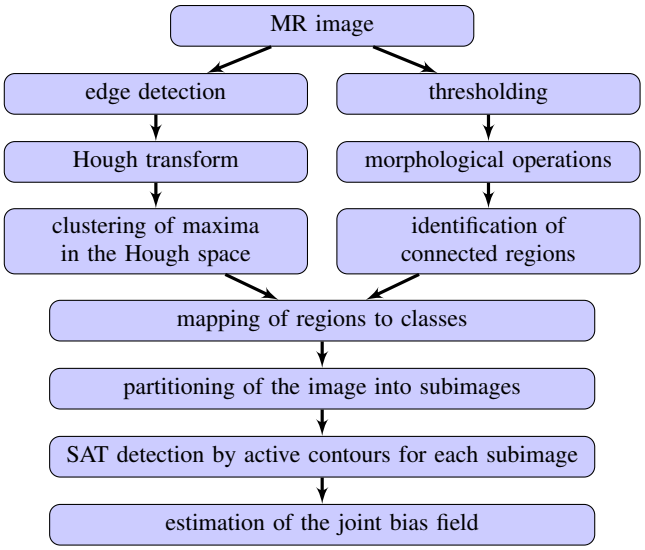

Fig. 1. Flow chart of the proposed algorithm for the fully automated object detection and compensation of IIH in MR images

straight lines [10], can be used to detect arbitrary curves, which can be described by an equation and a set of parameters [11]. The d parameters of the equation describing the object span a d-dimensional parameter space called Hough space. The parameters are usually quantized and have a limited range, so each parameter can take a limited number of possible values. Thus, it is possible to represent the Hough space by a so called voting matrix. Each point in the Hough space or rather each element of the d-dimensional voting matrix represents one possible object in the image space.

The Hough transform is usually applied to black and white edge images. For each edge pixel, the given equation is evaluated with all possible parameter combinations. Let $\boldsymbol{\omega}$ be the parameter vector and $\mathbf{x}_i$ the position of a foreground pixel. The equation describing the object is assumed to be $g(\boldsymbol{\omega}, \mathbf{x}_i) = 0$. The Hough transform of this pixel is then given by

$$\mathbf{H}_i(\boldsymbol{\omega}) = \begin{cases} 1 & \text{for } g(\boldsymbol{\omega}, \mathbf{x}_i) = 0 \\ 0 & \text{for } g(\boldsymbol{\omega}, \mathbf{x}_i) \neq 0 \end{cases} \tag{1}$$

for all $\boldsymbol{\omega}$.

The Hough transform of the complete edge image is a superposition of the transforms of the individual pixels:

$$\mathbf{H}(\boldsymbol{\omega}) = \sum_i \mathbf{H}_i(\boldsymbol{\omega}) \tag{2}$$

This means that for every possible parameter set $\boldsymbol{\omega}$, the Hough transform gives the number of pixels satisfying $g(\boldsymbol{\omega}, \mathbf{x}_i) = 0$. Thus, a high value in the Hough space means a high probability for the corresponding object $\boldsymbol{\omega}$.

A serious disadvantage of the Hough transform is its very high computational cost due to the brute force approach. The computational cost can be reduced by approximating the objects by circles instead of ellipses. But this still leads to a computation time of several minutes per image.

To overcome this difficulty, we change the point of view for the Hough transform: Instead of checking to which objects a particular pixel belongs, it is checked which pixels belong to a particular object. The Hough transform can then be formulated using the number

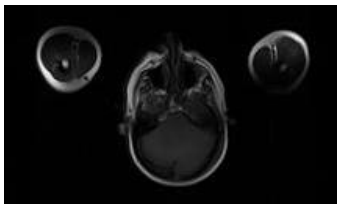

Fig. 2. MR image of a head and two upper arms with partially darkened SAT rings at the arms due to IIH

of pixels $\mathbf{x}$ satisfying $g(\boldsymbol{\omega}, \mathbf{x}_i) = 0$:

$$\mathbf{H}(\boldsymbol{\omega}) = |\{\mathbf{x} : g(\boldsymbol{\omega}, \mathbf{x}) = 0\}| \tag{3}$$

This leads to a much more efficient implementation using convolution, if the objects to be detected are translations of each other [12]. To detect all circles with a fixed radius r and different centers $\mathbf{c}$, the circular Hough transform can be expressed as a convolution of the image $I(\mathbf{x})$ with a kernel $G_r(\mathbf{x})$:

$$\mathbf{H}(\mathbf{c}, r) = \sum_{\mathbf{x}} I(\mathbf{x}) G_r(\mathbf{c} - \mathbf{x}), \quad G_r(\mathbf{x}) = \begin{cases} 1, & \|\mathbf{x}\| = r \\ 0, & \text{otherwise.} \end{cases} \tag{4}$$

By calculation of the convolution for all desired radii r, the Hough transform can be carried out very fast and efficiently.

2.2. Estimation of the number and position of the objects

As a high value in the Hough space corresponds to a high probability for the object given by the coordinates in the Hough space, the most likely objects can be found by determining the maxima in the Hough space. For a circular Hough transform, a circle in the image space leads to a clear maximum in the Hough space. However, cross sections of the human body are far from perfect circles. Since one object can be fitted by a lot of different segments of circles, they cause many different maxima with comparable values in the Hough space. This results in a large number of detected circle segments, see figure 3. If an image contains more than one object, the number and position of the objects can thus not be concluded directly from the maxima in the Hough space.

Because of the curvature of the edges, the centers of the circles usually lie within the objects. To find the number and the position of the objects, we therefore try to find clusters of the centers of the circles with high values in the voting matrix. As only the location of the circles is important for this task, the feature vector consists of the centers $\mathbf{c}$ of the circles. Only significant circles are considered, i.e. those corresponding to the 100 strongest local maxima in the voting matrix.

For the clustering of the circles, a modified version of the k-means algorithm is used. The k-means algorithm assigns N samples $\mathbf{c}_n$ to k clusters S_i and consists of a simple two-step procedure. The first step is the calculation of the class means $\boldsymbol{\mu}_i$ of the clusters S_i:

$$\boldsymbol{\mu}_i = \frac{1}{|S_i|} \sum_{\mathbf{c}_n \in S_i} \mathbf{c}_n \tag{5}$$

In the second step, a nearest mean classifier is used to assign the samples to the nearest class mean. Each sample $\mathbf{c}_n$ is assigned to exactly one class i by

$$\text{class of } \mathbf{c}_n = \arg\min_i \|\mathbf{c}_n - \boldsymbol{\mu}_i\| \tag{6}$$

These steps are repeated until there is no change in the second step. In its original form, the k-means algorithm needs the number of

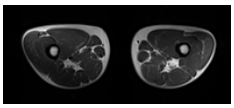

(a) Original image

(b) Edge image

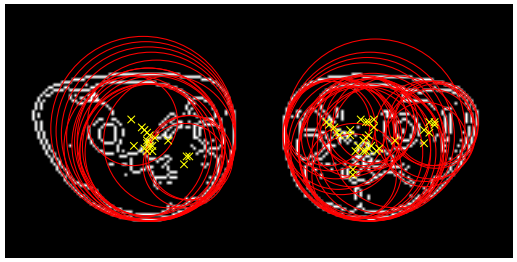

(c) 50 circles with the highest probability

Fig. 3. The 50 circles with the highest probability detected by the Hough transform of an edge-detected MR image of two thighs

classes and an initial guess for either the class means or the class assignments.

Because in this application the number of classes is unknown, the first step of the k-means algorithm was modified. If the minimum Euclidian distance between any two of the class means is smaller than a threshold ϑ, i.e.

$$\min_{i \neq j} \|\boldsymbol{\mu}_i - \boldsymbol{\mu}_j\| < \vartheta, \tag{7}$$

their classes are combined. The threshold ϑ was determined empirically as 1.5 times the average radius $\bar{r}$ of the clustered circles, i.e. $\vartheta = 1.5 \cdot \bar{r}$. Clearly, the threshold is linked to the mean object size. For small objects, the threshold is small enough not to merge the classes. If there is one big object, many classes will be merged.

As classes can be merged, but not splitted, the number of classes for the initial guess has to be chosen not too small. To gain a good initial guess, the following procedure is used: The circle $\mathbf{c}_m$ with the highest value in the voting matrix, which belongs to the set of not yet assigned circles S_0, is assigned to a new cluster S_i. All circles $\mathbf{c}_n$, whose center has a smaller distance to the center of $\mathbf{c}_m$ than 1.5 times this circle's radius r_m, are also assigned to S_i:

$$S_i = \{\mathbf{c}_n : \|\mathbf{c}_n - \mathbf{c}_m\| < 1.5 r_m \quad \forall \mathbf{c}_n \in S_0\} \tag{8}$$

This procedure is repeated until all circles are assigned to a class.

2.3. Partitioning of the image into subimages

To partition the image in a way that each subimage contains exactly one object, the borders between the subimages have to be very precise because some objects are only separated by a few pixels. The object contours therefore have to be considered for the partitioning. This is done by thresholding the image with an image dependent threshold computed by Otsu's method [1]. Subsequently, holes in the foreground regions are filled and small foreground regions are removed.

For every connected foreground region R_j, the centroid $\boldsymbol{\gamma}_j$ is calculated. Each region R_j is assigned to the class with the nearest mean $\boldsymbol{\mu}_i$ by

$$\text{class of } R_j = \arg\min_i \|\boldsymbol{\gamma}_j - \boldsymbol{\mu}_i\| \tag{9}$$

In this way, multiple regions belonging to the same object are linked to the same class. Figure 4a shows the class means $\boldsymbol{\mu}_i$ (marked by $+$) and region centroids $\boldsymbol{\gamma}_j$ (marked by $\times$) for the MR image depicted in figure 3a.

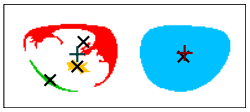

(a) Class means $\boldsymbol{\mu}_i$ ($+$) and region centroids $\boldsymbol{\gamma}_j$ ($\times$)

(b) Partitioned image

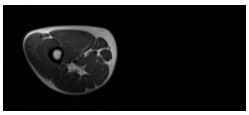

(c) Subimage

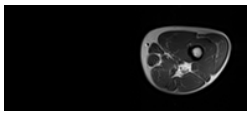

(d) Subimage

Fig. 4. Partitioning of the image into subimages

The image is partitioned into several big connected regions by assigning every background pixel to the class of the nearest foreground pixel. In figure 4b, the background pixels are depicted in a darker shade than the foreground regions they belong to. From each region, a new image is generated, which contains the original image in this region and is zero otherwise, see figures 4c and 4d.

3. TWO-STAGE APPROACH FOR THE DETECTION OF THE OBJECT BOUNDARY

The BC-FAT algorithm [9], which forms the basis of our proposed algorithm, uses active contours (also called snakes), to detect the SAT ring. A major issue with the active contours is the correct parametrization, because the choice of the parameters depends on the size and the shape of the object which is to be detected. So for different body parts, different parameters are needed for a reliable detection. Additionally, there is a trade-off between a fast and a precise adaption, if the initial contour is chosen too far away from the object boundary.

To overcome the latter problem, a two-scale approach is used. A fast adaption to the rough object boundary is carried out on a low scale, i.e. a low image resolution, and on a high scale, the rough estimate is refined.

The rough estimation of the object boundary is performed on an image resolution sampled down by a factor of four. In this stage, the parameters are chosen in a way that the emphasis lies on the internal energy of the snake, so that it stays fairly round, but quickly adapts to the object boundary. This rough estimation is then refined on the original resolution. The estimation of the previous stage is expanded in every direction by several pixels, to ensure that the snake is completely outside of the object. The enlarged contour is used as the initial contour of the second stage, which is parametrized so that the focus lies on the close adaption of the object boundary. Figure 5 shows the initial contour and the result of both stages for an MR image in the abdominal area.

By splitting the snake algorithm into a stage for the detection of the rough boundary and a stage for refinement, it was possible to find a set of parameters for each step, which could be used on all images regardless of the object size.

4. EVALUATION

The proposed algorithm for object detection was evaluated with 11 series of MR images. These series each consist of around 100 transversal cross-sectional images of the human body from the an-

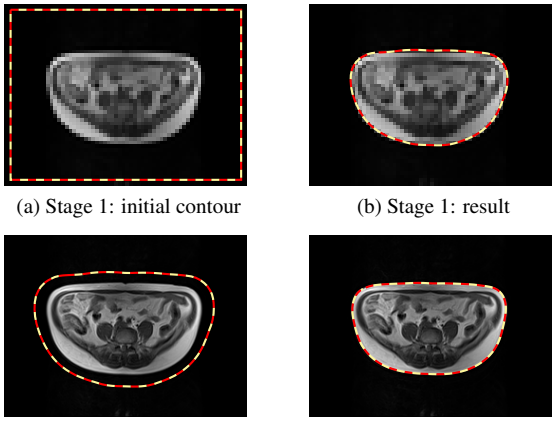

(a) Stage 1: initial contour (b) Stage 1: result

(c) Stage 2: initial contour (d) Stage 2: result

Fig. 5. Two-stage approach for the detection of the object boundary in an MR image in the abdominal area

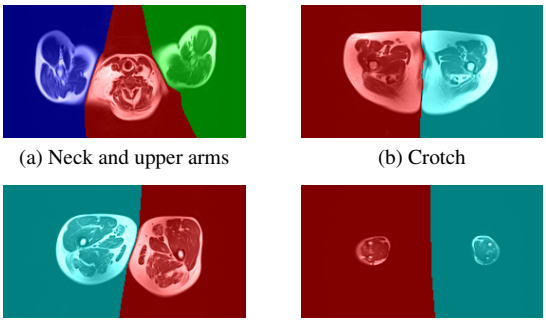

(a) Neck and upper arms (b) Crotch

(c) Thighs (d) Forearms

Fig. 6. Examples for a successful segmentation in difficult cases

kles to the wrists. Each slice has a thickness of 10 mm and a distance of 10 mm to the next slice.

In almost all cases, the segmentation worked correctly. Even in difficult areas like the shoulders or the crotch, where the number of objects changes, the correct number of objects was determined and the image was partitioned in a reasonable way. Figure 6 shows four examples of a successful segmentation even if the objects are very close together (a) - (c) or the SAT ring is very thin (d).

Errors in the segmentation can be grouped into four categories:

1. One of the objects was not detected.
2. Two objects were detected as one.
3. One object was detected as two objects.
4. The boundary between two regions crossed an object.

Errors of category 1 occur, if one of the objects is described by not one of the 100 strongest circles of the Hough transform. This can be the case, if one of the objects is significantly less round, e.g. less describable by circles, than the others.

The second kind of errors is caused by objects lying too close together, which leads to one big connected region after thresholding instead of two.

The thresholding is also the cause of errors of the third category. If one object is detected as multiple regions and the modified k-means leads to more than one class for this object, the regions belonging to the same object are assigned to different classes.

Errors of category 4 occur, when one of the objects has a very thin and darkened SAT ring. In some cases, large parts of this ring

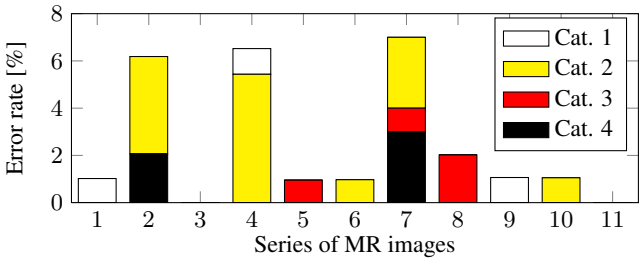

Fig. 7. Error rates for each series and each error category

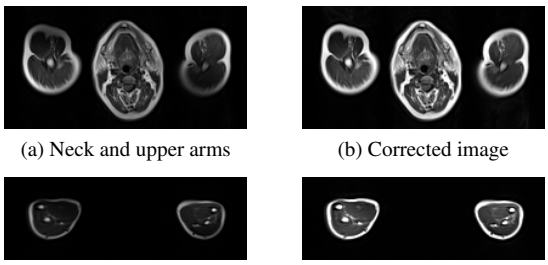

(a) Neck and upper arms (b) Corrected image

(c) Forearms (d) Corrected image

Fig. 8. Successful correction of intensity inhomogeneities with multiple objects

may not be detected as foreground by the thresholding, so that the object is only described by a ring segment. The boundary between this and another object can then cross the object in the area, where the SAT ring was not detected.

The error rate for each series and each category is depicted in figure 7. Multiple errors of the same category (in series 2, 4, 7 and 8) occur on adjacent images, because they have very similar characteristics. Most errors belong to category 2 and appear in pictures of thighs touching each other. Errors of category 4 only appeared in pictures of the head and upper arms, where the head was not detected correctly because of the very thin SAT ring.

For the correction of the bias field, only a qualitative evaluation could be carried out, because a groundtruth does not exist. By using the two-stage procedure described in section 2, in most cases, the SAT ring was detected successfully. Even for objects with a very thin SAT ring such as forearms, the ring was detected. The SAT ring could not be detected reliably, when the partitioning of the image was incorrect or when too many motion artifacts were present.

If the detection of the SAT ring was successful, the correction of the bias field showed good results as well. After the correction, the brightness of the SAT rings shows almost no fluctuation and also the visceral adipose tissue shows the same brightness. Figure 8 shows that the inhomogeneity correction for multiple objects works even in cases where the SAT ring is smeared (b) or very thin (d).

5. CONCLUSION

We presented a reliable algorithm to segment cross-sectional MR images for the whole body into subimages, each containing one object. This algorithm is mainly based on the circular Hough transform and a modified k-means clustering. We showed that by using a two-scale approach for the active contours, these can be applied to objects of arbitrary size without adjusting the parameters. In this way, a fully automated correction of inhomogeneities in cross-sectional MR images for the whole body is possible by means of the BC-FAT algorithm.

6. REFERENCES

[1] Nobuyuki Otsu, "A threshold selection method from grey level histograms," *IEEE Transactions on Systems, Man, and Cybernetics*, vol. 9, no. 1, pp. 62–66, 1979.

[2] Michael Kass, Andrew Witkin, and Demetri Terzopoulos, "Snakes: Active contour models," *International Journal of Computer Vision*, vol. 1, pp. 321–331, 1988.

[3] R. Malladi, J.A. Sethian, and B.C. Vemuri, "Shape modeling with front propagation: a level set approach," *Pattern Analysis and Machine Intelligence, IEEE Transactions on*, vol. 17, no. 2, pp. 158 –175, Feb 1995.

[4] L. Axel, J. Costantini, and J. Listerud, "Intensity correction in surface-coil MR imaging," *American Journal of Roentgenology*, vol. 148, no. 2, pp. 418–420, 1987.

[5] A.W.C. Liew and Hong Yan, "An adaptive spatial fuzzy clustering algorithm for 3-D MR image segmentation," *Medical Imaging, IEEE Transactions on*, vol. 22, no. 9, pp. 1063 –1075, Sept. 2003.

[6] D.L. Pham and J.L. Prince, "Adaptive fuzzy segmentation of magnetic resonance images," *Medical Imaging, IEEE Transactions on*, vol. 18, no. 9, pp. 737 –752, Sept. 1999.

[7] O. Salvado, C. Hillenbrand, Shaoxiang Zhang, and D.L. Wilson, "Method to correct intensity inhomogeneity in MR images for atherosclerosis characterization," *Medical Imaging, IEEE Transactions on*, vol. 25, no. 5, pp. 539 –552, May 2006.

[8] Chunming Li, Chenyang Xu, Adam W. Anderson, and John C. Gore, "MRI tissue classification and bias field estimation based on coherent local intensity clustering: A unified energy minimization framework," in *Proceedings of the 21st International Conference on Information Processing in Medical Imaging*, 2009, pp. 288–299.

[9] Christian Würslin, Fabian Springer, Bin Yang, and Fritz Schick, "Compensation of RF field and receiver coil induced inhomogeneity effects in abdominal MR images by a priori knowledge on the human adipose tissue distribution," *Journal of Magnetic Resonance Imaging*, vol. 34, no. 3, pp. 716–726, 2011.

[10] P. V. C. Hough, "Method and means for recognizing complex patterns," US Patent 3069654, 1962.

[11] R. O. Duda and P. E. Hart, "Use of the Hough transformation to detect lines and curves in pictures," *Commun. ACM*, vol. 15, no. 1, pp. 11–15, 1972.

[12] J. Sklansky, "On the Hough technique for curve detection," *IEEE Transactions on Computers*, vol. 27, pp. 923–926, 1978.